Interplay between Raman shift and thermal expansion in graphene: Temperature-dependent measurements and analysis of substrate corrections

S. Linas,[*,†] Y. Magnin,[*,‡] B. Poinsot, O. Boisron, G. D. Förster, V. Martinez, R. Fulcrand, F. Tournus, V. Dupuis, F. Rabilloud, and L. Bardotti
ILM, Université Lyon 1 and CNRS UMR5306, 10 rue Ada Byron, 69622 Villeurbanne Cedex, France

Z. Han, D. Kalita, and V. Bouchiat
Institut Néel, CNRS UPR2940 and Université Grenoble 1, Alpes, 25 rue des Martyrs, 38042 Grenoble, France

F. Calvo
LIPhy, Université Grenoble 1 and CNRS, UMR5588, 140 avenue de la physique, 38402 St. Martin d'Hères, France
(Received 28 November 2014; revised manuscript received 28 January 2015; published 24 February 2015)

Measurements and calculations have shown significant disagreement regarding the sign and temperature variations of the thermal expansion coefficient (TEC) of graphene $\alpha(T)$. Here we report dedicated Raman scattering experiments conducted for graphene monolayers deposited on silicon nitride substrates and over a broad temperature range extending over 150–800 K. The relation between those measurements for the G band and the graphene TEC, which involves correcting the measured signal from the mismatch contribution of the substrate, is analyzed based on different theoretical candidates for $\alpha(T)$. Contrary to calculations in the quasiharmonic approximation, a many-body potential reparametrized for graphene correctly reproduces experimental data, suggesting that the TEC is more likely to be positive above room temperature.

DOI: 10.1103/PhysRevB.91.075426 PACS number(s): 65.80.Ck, 68.65.Pq, 63.22.Rc, 65.40.De

I. INTRODUCTION

The thermal expansion coefficient (TEC) of materials involved in solid interfaces is a key parameter characterizing the stress within the materials, which in turn can modulate their electronic properties [1]. The use of graphene in high-density, integrated electronic devices [2–4] or as matrix reinforcement for composite materials [5] would benefit from better knowledge of the TEC, in particular its dependence on temperature $\alpha(T)$.

Unfortunately, experiment and theory show markedly diverse results regarding the TEC of graphene. The scanning electronic microscopy (SEM) measurements carried by Bao *et al.* [6] found negative values for α at low temperature and a sign change at around 350 K. Based on Raman scattering experiments, Yoon *et al.* [7] also found negative TEC but did not find evidence for a sign change up to 400 K. Negative coefficients were also obtained by Singh *et al.* [8], who used a nanoelectromechanical resonator. In both Refs. [7,8] strong variations among samples were emphasized. On the theory side, density-functional perturbation theory (DFPT) [9] and *ab initio* molecular dynamics [10] predicted an all-negative α in a broad temperature range, whereas nonequilibrium Green's function calculations [11] found a sign change near 600 K. Atomistic Monte Carlo (MC) simulations have found all-positive, all-negative, or sign-changing variations of the TEC depending on the potential used [12,13]. This diversity of behaviors is related to the importance of anharmonicities [14] and the difficulty of describing them properly in relation to the measurements.

Raman spectroscopy in a broad temperature range is one of the indirect ways to access such properties. Being a fast and nondestructive tool that can offer structural and electronic information, it has been widely used in the recent years for the characterization of graphene [15–20]. In particular, from such measurements the number of layers, density of defects, amount of stress, and doping can all be evaluated [15–20]. As a direct probe of the phonon structure, temperature-dependent measurements should be indirectly related to the lattice parameter and hence to the TEC. However, in experiments graphene is held on (or by) a substrate, and it is well known that the detailed graphene structure is sensitive to the nature of the support [21]. In particular, incommensurability between the two lattices gives rise to strain often manifested by corrugation [22], which could affect the measured TEC [23]. More generally, the contact between the two materials with different thermal expansion coefficients is a source of strain [7]. Even though some authors have disregarded this correction in their measurements [6], the importance of substrate interactions on the TEC has been recognized before [11].

One limitation of earlier investigations is the rather restricted temperature ranges over which the measurements were conducted, generally below 400 K. In the present work, we have extended this range to a higher upper limit extending above 800 K. More importantly, we have carried out a comprehensive analysis of the Raman G band based on underlying models for the graphene TEC, carefully disentangling the contribution of the substrate by following the phenomenological procedure laid out by Yoon *et al.* [7]. Our experimental results are found to be incompatible with TECs that remain negative in the entire temperature range but agree

[*]These authors contributed equally to this work.
[†]Present address: LMI, Université Lyon 1 and CNRS UMR5615, 43 boulevard du 11 Novembre 1918, 69622 Villeurbanne Cedex, France
[‡]Present address: CINaM, CNRS and Aix-Marseille University, Campus de Luminy, Case 913, 13288 Marseille, France.

reasonably well with an all-positive model TEC predicted by a dedicated atomistic potential precisely fitted to reproduce the phonon structure of graphene.

II. EXPERIMENTS

Strictly monolayer graphene was synthesized on a copper foil (25 μm thick, 99.8% purity, Alfa Aesar) by a pulsed chemical vapor deposition (CVD) growth method [24]. After the foil was etched in a $(NH_4)_2S_2O_8$ solution at 5×10^{-2} mol/L concentration, the graphene sheet was directly transferred on a SiN membrane (thickness 50 nm) supported on a silicon substrate (Silson) using a resist-free technique [25]. Before experiments, the samples were annealed *in situ* at 600 K in an inert atmosphere. The measurements were carried out using two distinct Raman setups. First, a Renishaw RM 1000 micro-Raman spectrometer equipped with a 1800 lines/mm grating used a laser power kept low enough not to induce any shift of the G peak. A 50× long-working-distance objective was used, and the samples were heated and cooled in a Linkam THMSG600 under ultrapure Ar (ALPHAGAZ 2, Air Liquide) atmosphere. A second homemade Raman setup was adapted to an ultrahigh vacuum (UHV) chamber (base pressure 10^{-9} mbar) and a Horiba spectrometer (TRIAX320). The excitation wavelength was set to 532 nm in both experiments. The G and $2D$ peaks were fitted to single Lorentzians for analysis. Additional SEM imaging was performed after the Raman measurements in a FEI Nova NanoSEM 450 microscope at an acceleration voltage of 5 kV and with a sample tilted at 45° with respect to the electron beam.

III. RESULTS AND DISCUSSION

Figure 1(a) schematically depicts the graphene sample supported on the SiN/Si substrate, and Fig. 1(b) shows a SEM micrograph including the Raman laser spot. While grain boundaries finer than micrometer sizes can be evidenced by microscopy [26], the graphene samples used in the present work were shown to be monocrystalline over dimensions exceeding 10 μm [24]. A typical Raman spectrum represented in the inset of Fig. 1(c) shows symmetric Lorentzian line shapes for the $2D$ peak and an intensity ratio $I_{2D}/I_G \sim 1.5$ with the G peak, both features being consistent with a single graphene layer [16]. In addition, the low ratio I_D/I_G with the D peak suggests a low density of defects [16]. The variations of the G peak frequency $\omega_G(T)$ with increasing temperature are shown in Fig. 1(c) for a sample in argon atmosphere. These reasonably smooth variations, together with the SEM data, indicate that the graphene layer does not present significant folded areas, cracks, or wrinkles, at least in the area probed by the laser. Additional measurements were performed on other samples and under UHV or argon atmosphere and show comparable results [27].

The room-temperature value of ω_G found for our sample (1587.2 cm^{-1}) is slightly shifted compared to the intrinsic value of 1581.6 cm^{-1} expected for charge- and strain-free graphene [18], suggesting some doping and strain in our sample. The small discontinuities of 1–2 cm^{-1} observed for $\omega_G(T)$ might originate from a stick-slip of the graphene layer on the nitride surface, which is also visible in the measurements of Calizo and coworkers on silica substrates [28]. Between 100 and 400 K the temperature variations of ω_G are roughly linear with a slope of $-0.023\ cm^{-1}\ K^{-1}$, in fair agreement with values reported previously for graphene deposited on silica substrates ($-0.016\ cm^{-1}\ K^{-1}$ in Ref. [28], $-0.05\ cm^{-1}\ K^{-1}$ in Ref. [7]).

The observed thermal contribution to the Raman frequency shift of the G peak, $\Delta\omega_G(T)$, was evaluated by removing from $\omega_G(T)$ the value extrapolated at 0 K using a polynomial fit, $\omega_G(T = T_0 \simeq 0) = 1591\ cm^{-1}$ (note that this fit serves no purpose other than extrapolating to the T_0 reference temperature). To determine the intrinsic Raman shift of the bare graphene layer, the contribution $\Delta\omega_G^S(T)$ of the substrate-induced strain was removed from $\Delta\omega_G(T)$ following the same procedure advocated by Yoon *et al.* [7] based on the TECs of both graphene and substrate,

$$\Delta\omega_G^S(T) = \beta\varepsilon(T) = \beta\int_{T_0}^{T}[\alpha_{\rm sub}(T) - \alpha_{\rm gr}(T)]dT. \qquad (1)$$

In the previous equation we have denoted the strain experienced by the graphene layer on its substrate by $\varepsilon(T)$ and the TECs of the substrate and of the graphene layer by $\alpha_{\rm sub}$ and $\alpha_{\rm gr}$, respectively. β is the biaxial strain coefficient of the G band known to be approximately [29,30] $\beta = -70 \pm 3\ cm^{-1}/\%$. Equation (1) is central to our analysis as it provides a relation between the experimentally measured Raman signal and the graphene TEC we aim to discuss. To evaluate the substrate contribution to the Raman signal it is necessary to integrate the thermal expansion coefficients of the two materials over temperature. The TEC $\alpha_{\rm sub}$ of the SiN substrate was taken from the literature [31] and was extrapolated down to low temperatures $T < 400$ K using data known for the similar Si_3N_4 system [32].

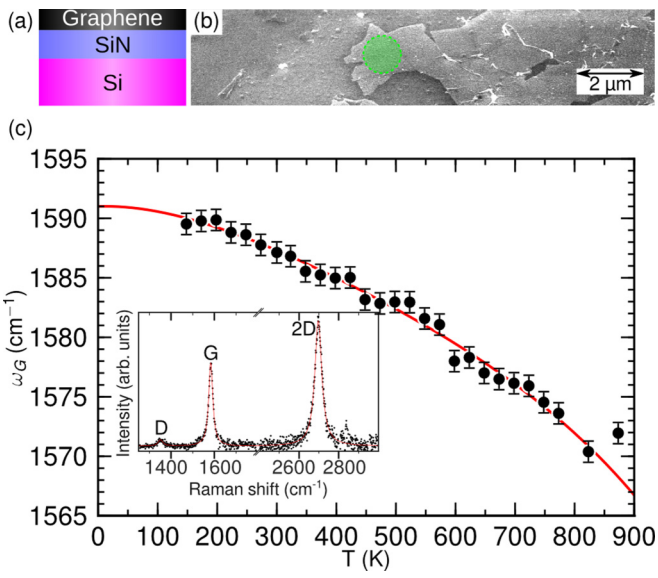

FIG. 1. (Color online) (a) Schematic of the sample, a single-layer graphene film grown by CVD and transferred on a SiN/Si substrate. (b) Scanning electron micrograph of the sample, with the probed area being highlighted by a green dashed circle. (c) G peak frequency ω_G (symbols) fitted down to 0 K using a fourth-order polynomial (red line). The inset shows a typical Raman spectrum at $T = 300$ K (black circles) and Lorentzian fits of the D, G, and $2D$ peaks (red lines).

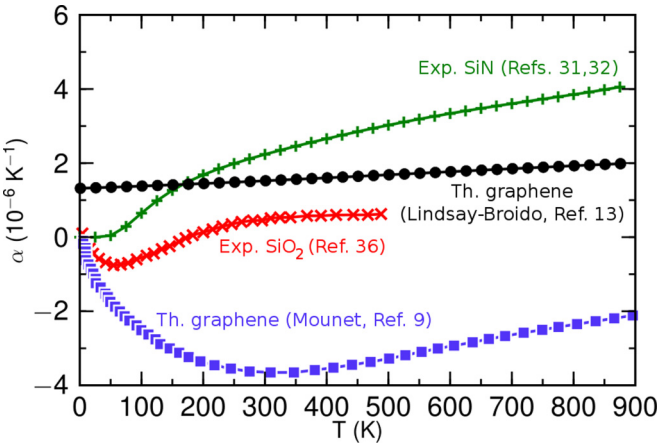

FIG. 2. (Color online) Temperature dependence of the experimental thermal expansion coefficients α of silicon nitride (green pluses) and silica (red crosses) and theoretical in-plane coefficients of graphene obtained by Mounet and Marzari in the quasiharmonic approximation (blue squares) and from classical MC simulations based on the Lindsay-Broido reparametrization of the Tersoff bond-order potential for graphene (black circles).

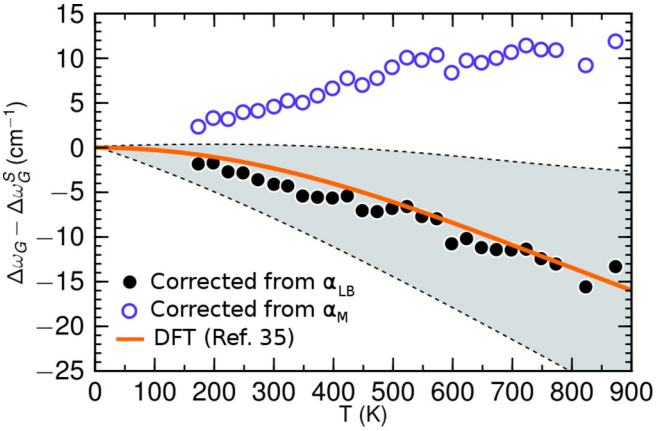

FIG. 3. (Color online) Temperature dependence of the Raman G band shift of pure graphene, corrected from the substrate mismatch contribution using different model TEC α_{gr}, namely, the quasiharmonic Mounet-Marzari model (α_M, open circles) and the Lindsay-Broido semiempirical model (α_{LB}, solid circles). The shaded area corresponds to varying the α_{LB} function by $\pm 2 \times 10^{-6}\,K^{-1}$, and the solid line shows the Raman shift calculated by Bonini and coworkers [35] from DFT.

For graphene, several forms were tried for $\alpha_{gr}(T)$ in the hope that comparison with experiment would ultimately settle generic conclusions about the expected features of this fundamental quantity. The DFPT results from Mounet and Marzari [9] were chosen as a representative of the quasiharmonic approximation based on first-principles data, giving a TEC that we denote as α_M and that is entirely negative in the relevant temperature range. Alternatively, among the various predictions of fully anharmonic MC simulations based on atomistic potentials [13], we have chosen those obtained with a recent reparametrization of the Tersoff bond-order potential [33] by Lindsay and Broido [34] dedicated to graphene and denoted as α_{LB}. The variations of the two aforementioned thermal expansion coefficients with temperature are shown in Fig. 2. The strong discrepancies between the two model TECs for graphene are expected to convey to the Raman shift, and we have reported in Fig. 3 the variations of $\Delta\omega_G(T)$ obtained by integrating Eq. (1) with the corresponding functions $\alpha_{gr} = \alpha_M$ and α_{LB}. In order to compare the relative performances of the two models, a third set of reference data is required, which is provided by the theoretical Raman shift of freestanding graphene calculated by Bonini and coworkers [35] using density-functional theory (DFT) calculations under appropriate anharmonic expansions. This purely theoretical result, also depicted in Fig. 3, clearly agrees quantitatively with the present measurements if the substrate correction originates from the Lindsay-Broido model but disagrees otherwise. It is important to evaluate the sensitivity of this result to the α_{gr} ingredient, and we have repeated the integration using the α_{LB} model but shifting it by $\pm 2 \times 10^{-6}\,K^{-1}$ in the entire temperature range, a negative shift leading to a negative TEC at low temperature and a sign change near 400 K. The resulting Raman shift of the G band also varies (see Fig. 3) but remains closer to the reference DFT data than the values obtained with the α_M correction. This observation puts some constraints on the true α_{gr} function.

According to the present measurements and analysis, the graphene TEC is better described by the Lindsay-Broido model than the Mounet-Marzari quasiharmonic model. Those conclusions can be challenged by considering the case of silica substrates, on which earlier Raman measurements were performed [7,28]. Two sets of experimental data were taken from the works of Yoon and coworkers [7] and Calizo *et al.* [28] and were subject to the same correcting treatment as performed here for silicon nitride but using the experimental thermal expansion coefficient of silica [36] also superimposed in Fig. 2. From these two data sets for $\Delta\omega_G(T)$, the correction $\Delta\omega_G^S(T)$ was calculated from the two graphene model TECs α_M and α_{LB}, and the results are again compared to the reference DFT results of Bonini and coworkers [35] in Fig. 4. Correcting the data by Yoon *et al.* with the Mounet-Marzari model for α_{gr} leads to values for the Raman shift as obtained in Ref. [7]. They are significantly closer to the DFT reference data than those obtained with the all-positive TEC predicted by the Lindsay-Broido model, although the agreement is never excellent. Incidentally, we note that Yoon and coworkers had to significantly adjust the input $\alpha_{gr}(T)$ in order to get an even better agreement. However, the opposite observations can be made when the calculations are performed using the experimental data from Calizo *et al.* [28], and a fully negative model for α_{gr} markedly underestimates the Raman shift, while the Lindsay-Broido model yields reasonable agreement. Given the significant dispersion among experimental measurements for graphene on SiO_2 substrates [7,28] and, in particular, the much more limited temperature range on which these measurements were conducted, it seems difficult to conclude unambiguously about the sign and variations of the TEC based on the silica data alone. In contrast, the present data obtained on silicon nitride display better overall agreement with theoretical models.

The discrepancies between the predictions of the Mounet-Marzari and Lindsay-Broido corrections are related to the

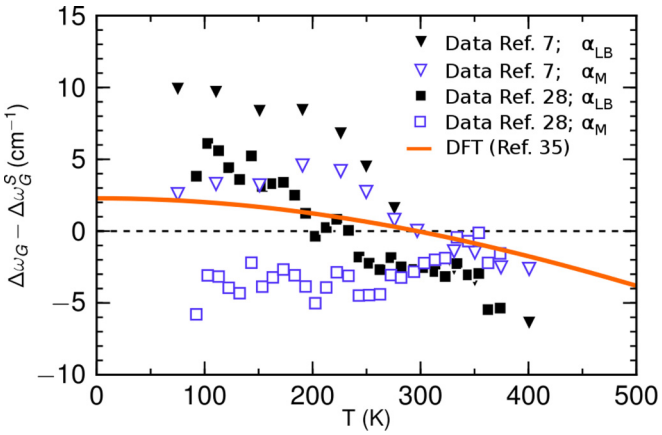

FIG. 4. (Color online) Temperature dependence of the Raman G band shift of pure graphene from measurements on the SiO_2 substrate, as measured by Yoon *et al.* [7] (triangles) and by Calizo *et al.* [28] (squares) and corrected for the substrate mismatch contribution using the Mounet-Marzari (α_M, open symbols) and Lindsay-Broido (α_{LB}, solid symbols) models. The solid line shows the Raman shift determined by Bonini and coworkers [35] from DFT calculations, shifted to cross the vertical axis at 297 K.

rather different natures of the two models, with the former quasiharmonic model [9] being expected to be better at low temperature, while the latter anharmonic but classical model [34] was adjusted for room-temperature properties. Neither model was fitted to reproduce temperature-dependent properties; hence it is also unclear to what extent they would be able to correctly capture anharmonicities, especially above room temperature. In the absence of independent measurements and in view of the major diversity among computational models [13], it is tempting to conclude that the true thermal expansion coefficient lies somewhere between the two models and hence that it must at least be positive above some temperature close to 300 K.

IV. CONCLUDING REMARKS

We have performed Raman scattering measurements of graphene monolayers supported on silicon nitride over an extended temperature range and used these data to establish some constraints on the TEC of bare graphene. Our analysis relies on the correction to the measured Raman shift of the G band due to the mismatch contribution from the substrate and on the comparison of the corrected signal to benchmark anharmonic DFT calculations [35]. The present approach, which follows earlier efforts by other authors [7], requires knowledge of the expansion coefficients of both graphene and substrate materials. A model TEC based on finite-temperature MC simulations with a potential dedicated to graphene turned out to reproduce the experimental data best, suggesting that the TEC is more likely to be positive above moderate temperatures. Until more direct measurements are carried out, one main outcome of the present work has been to shed more light on the importance of the substrate, not only in altering the properties of deposited graphene but also on the nature and magnitude of the corrections inferred from available data.

The incompatibility between the present conclusions regarding the sign of the TEC and earlier conclusions [7] could have different possible causes. The role of strain and doping in our experimental sample, manifested by a deviation exceeding 5 cm^{-1} in the room-temperature value, was assumed not to depend markedly on temperature throughout our analysis. However, strain effects could be more important, as notably suggested by Yu and coworkers [17]. The Raman signal is also sensitive to the amount of unintentional doping by the substrate [18], and this effect, which is likely to be temperature dependent, should be incorporated as well. As far as the analysis of experimental data is concerned, the use of a linear equation relating the stress to the Raman shift might be oversimplified, and the perturbative calculations of Bonini and coworkers [35] on which the entire analysis relies may break down at moderate temperatures. Finally, atomistic simulations themselves could be improved at low temperature by incorporating quantum-mechanical effects, possibly through the use of the path-integral description of nuclear motion.

It would be valuable to exploit other Raman signals such as the $2D$ peak as an alternative to the G band, even though a theoretical reference for comparison is currently lacking. Future work could be devoted to extending the present methodology to other two-dimensional or layered materials such as hexagonal boron nitride or to transition-metal dichalcogenides, which currently hold promise as a result of their interesting semiconductor properties [37].

ACKNOWLEDGMENTS

The authors gratefully acknowledge the CECOMO (Université Lyon 1) for providing access to the Raman spectroscopy facilities and C. Albin (ILM, PLYRA). Research was supported by ANR (France), Project No. ANR-2010-BLAN-1019-NMGEM.

[1] Z. H. Ni, T. Yu, Y. H. Lu, Y. Y. Wang, Y. P. Feng, and Z. X. Shen, Uniaxial strain on graphene: Raman spectroscopy study and band-gap opening, ACS Nano **2**, 2301 (2008).

[2] K. S. Novoselov, A. K. Geim, S. V. Morozov, D. Jiang, Y. Zhang, S. V. Dubonos, I. V. Grigorieva, and A. A. Firsov, Electric field effect in atomically thin carbon films, Science **306**, 666 (2004).

[3] Y. Zhang, Y.-W. Tan, H. L. Stormer, and P. Kim, Experimental observation of the quantum Hall effect and Berry's phase in graphene, Nature (London) **438**, 201 (2005).

[4] K. I. Bolotin, K. J. Sikes, Z. Jiang, M. Klima, G. Fudenberg, J. Hone, P. Kim, and H. L. Stormer, Ultrahigh electron mobility in suspended graphene, Solid State Commun. **146**, 351 (2008).

[5] S. Stankovich, D. A. Dikin, G. H. B. Dommett, K. M. Kohlhaas, E. J. Zimney, E. A. Stach, R. D. Piner, S. T. Nguyen, and R. S. Ruoff, Graphene-based composite materials, Nature (London) **442**, 282 (2006).

[6] W. Bao, F. Miao, Z. Chen, H. Zhang, W. Jang, C. Dames, and C. N. Lau, Controlled ripple texturing of suspended graphene and ultrathin graphite membranes, Nat. Nanotechnol. **4**, 562 (2009).

[7] D. Yoon, Y.-W. Son, and H. Cheong, Negative thermal expansion coefficient of graphene measured by Raman spectroscopy, Nano Lett. **11**, 3227 (2011).

[8] V. Singh, S. Sengupta, H. S. Solanki, R. Dhall, A. Allain, S. Dhara, P. Pant, and M. M. Deshmukh, Probing thermal expansion of graphene and modal dispersion at low-temperature using graphene nanoelectromechanical systems resonators, Nanotechnology **21**, 165204 (2010).

[9] N. Mounet and N. Marzari, First-principles determination of the structural, vibrational and thermodynamic properties of diamond, graphite, and derivatives, Phys. Rev. B **71**, 205214 (2005).

[10] M. Pozzo, D. Alfè, P. Lacovig, P. Hofmann, S. Lizzit, and A. Baraldi, Thermal expansion of supported and freestanding graphene: Lattice constant versus interatomic distance, Phys. Rev. Lett. **106**, 135501 (2011).

[11] J. W. Jiang, J. S. Wang, and B. Li, Thermal expansion in single-walled carbon nanotubes and graphene: Nonequilibrium green's function approach, Phys. Rev. B **80**, 205429 (2009).

[12] K. V. Zakharchenko, A. Fasolino, J. H. Los, and M. I. Katsnelson, Melting of graphene: From two to one dimension, J. Phys. Condens. Matter **23**, 202202 (2011).

[13] Y. Magnin, G. D. Förster, F. Rabilloud, F. Calvo, A. Zappelli, and C. Bichara, Thermal expansion of free-standing graphene: Benchmarking semi-empirical potentials, J. Phys. Condens. Matter **26**, 185401 (2014).

[14] A. Fasolino, J. H. Los, and M. I. Katsnelson, Intrinsic ripples in graphene, Nat. Mater. **6**, 858 (2007).

[15] A. C. Ferrari, J. C. Meyer, V. Scardaci, C. Casiraghi, M. Lazzeri, F. Mauri, S. Piscanec, D. Jiang, K. S. Novoselov, S. Roth, and A. K. Geim, Raman spectrum of graphene and graphene layers, Phys. Rev. Lett. **97**, 187401 (2006).

[16] A. C. Ferrari and D. M. Basko, Raman spectroscopy as a versatile tool for studying the properties of graphene, Nat. Nanotechnol. **8**, 235 (2013).

[17] V. Yu, E. Whiteway, J. Maassen, and M. Hilke, Raman spectroscopy of the internal strain of a graphene layer grown on copper tuned by chemical vapor deposition, Phys. Rev. B **84**, 205407 (2011).

[18] J. E. Lee, G. Ahn, J. Shim, Y. S. Lee, and S. Ryu, Optical separation of mechanical strain from charge doping in graphene, Nat. Commun. **3**, 1024 (2012).

[19] W.-G. Xie, X. Lai, X.-M. Wang, X. Wan, M.-L. Yan, W.-J. Mai, P.-Y. Liu, J. Chen, and J. Xu, Influence of annealing on raman spectrum of graphene in different gaseous environments, Spectrosc. Lett. **47**, 465 (2014).

[20] H. Zhou, C. Qiu, F. Yu, H. Yang, M. Chen, L. Hu, Y. Guo, and L. Sun, Raman scattering of monolayer graphene: The temperature and oxygen doping effects, J. Phys. D **44**, 185404 (2011).

[21] C. Soldano, A. Mahmood, and E. Dujardin, Production, properties and potential of graphene, Carbon **48**, 2127 (2010).

[22] A. B. Preobrajenski, M. L. Ng, A. S. Vinogradov, and N. Martensson, Controlling graphene corrugation on lattice-mismatched substrates, Phys. Rev. B **78**, 073401 (2008).

[23] F. Jean, T. Zhou, N. Blanc, R. Felici, J. Coraux, and G. Renaud, Effect of preparation on the commensurabilities and thermal expansion of graphene on Ir(111) between 10 and 1300 K, Phys. Rev. B **88**, 165406 (2013).

[24] Z. Han, A. Kimouche, D. Kalita, A. Allain, H. Arjmandi-Tash, A. Reserbat-Plantey, L. Marty, S. Pairis, V. Reita, N. Bendiab, J. Coraux, and V. Bouchiat, Homogeneous optical and electronic properties of graphene due to the suppression of multilayer patches during CVD on copper foils, Adv. Funct. Mater. **24**, 964 (2014).

[25] K. S. Kim, Y. Zhao, H. Jang, S. Y. Lee, J. M. Kim, K. S. Kim, J.-H. Ahn, P. Kim, J.-Y. Choi, and B. H. Hong, Large-scale pattern growth of graphene films for stretchable transparent electrodes, Nature (London) **457**, 706 (2009).

[26] S. U. Yu, Y. Cho, B. Park, N. Kim, I. S. Youn, M. Son, J. K. Kim, H. C. Choi, and K. S. Kim, Fast benchtop visualization of graphene grain boundaries using adhesive properties of defects, Chem. Commun. **49**, 5474 (2013).

[27] See Supplemental Material at http://link.aps.org/supplemental/10.1103/PhysRevB.91.075426 for additional Raman spectroscopy measurements.

[28] I. Calizo, A. A. Balandin, W. Bao, F. Miao, and C. N. Lau, Temperature dependence of the raman spectra of graphene and graphene multilayers, Nano Lett. **7**, 2645 (2007).

[29] T. M. G. Mohiuddin, A. Lombardo, R. R. Nair, A. Bonetti, G. Savini, R. Jalil, N. Bonini, D. M. Basko, C. Galiotis, N. Marzari, K. S. Novoselov, A. K. Geim, and A. C. Ferrari, Uniaxial strain in graphene by raman spectroscopy: G peak splitting, Grüneisen parameters, and sample orientation, Phys. Rev. B **79**, 205433 (2009).

[30] D. Yoon, Y.-W. Son, and H. Cheong, Strain-dependent splitting of the double-resonance raman scattering band in graphene, Phys. Rev. Lett. **106**, 155502 (2011).

[31] A. K. Sinha, H. J. Levinstein, and T. E. Smith, Thermal stresses and cracking resistance of dielectric films (SiN, Si_3N_4, and SiO_2) on Si substrates, J. Appl. Phys. **49**, 2423 (1978).

[32] W. Paszkowicz, R. Minikayev, P. Piszora, M. Knapp, C. Bähtz, J. M. Recio, M. Marqués, P. Mori-Sánchez, L. Gerward, and J. Z. Jiang, Thermal expansion of spinel-type Si_3N_4, Phys. Rev. B **69**, 052103 (2004).

[33] J. Tersoff, New empirical approach for the structure and energy of covalent systems, Phys. Rev. B **37**, 6991 (1988).

[34] L. Lindsay and D. A. Broido, Optimized Tersoff and Brenner empirical potential parameters for lattice dynamics and phonon thermal transport in carbon nanotubes and graphene, Phys. Rev. B **81**, 205441 (2010).

[35] N. Bonini, M. Lazzeri, N. Marzari, and F. Mauri, Phonon Anharmonicities in graphite and graphene, Phys. Rev. Lett. **99**, 176802 (2007).

[36] NIST, Standard Reference Material 739 Certificate, 1991.

[37] Q. H. Wang, K. Kalantar-Zadeh, A. Kis, J. N. Coleman, and M. S. Strano, Electronics and optoelectronics of two-dimensional transition metal dichalcogenides, Nat. Nanotechnol. **7**, 699 (2012).